Investigation on the Fracture Behavior and Morphology of Maleated Poly(ethylene 1-octene) Toughened and Glass Fiber-Reinforced Nylon 1010

Haiyang Yu, Yong Zhang, Wentan Ren

State Key Laboratory of Metal Matrix Composites, School of Chemistry and Chemical Technology, Shanghai Jiao Tong University, Shanghai 200240, China

Received 18 May 2008; accepted 18 October 2008
DOI 10.1002/app.29531
Published online 16 March 2009 in Wiley InterScience (www.interscience.wiley.com).

ABSTRACT: The maleated poly(ethylene 1-octene) (POE-*g*-MAH)-toughened and glass fiber (GF)-reinforced nylon 1010 was prepared by melting extrusion. A good trade-off between stiffness and toughness was obtained by the combination of POE-*g*-MAH and GF. The essential work of fracture (EWF) model was used to characterize the fracture behavior of nylon/POE-*g*-MAH/GF composites. With increasing GF content, the energy consumed in outer plastic zone gradually decreased, and the work consumed in inner fracture process zone reached the maximum value at the GF content of 10 wt %. Morphology investigations showed that POE-*g*-MAH was uniformly dispersed in nylon/POE-*g*-MAH (80/20) blend, and the nylon around POE-*g*-MAH particles suffered a great plastic deformation in the impact test. For nylon/POE-*g*-MAH/GF composites, large plastic deformation occurred in the matrix around GF rather than around rubber particles. Dynamic mechanical analysis showed that GF significantly increased the storage and loss moduli and decreased value of tan δ, but had little effect on its position. © 2009 Wiley Periodicals, Inc. J Appl Polym Sci 113: 181–189, 2009

Key words: nylon; toughness; stiffness; fracture

INTRODUCTION

Nylon 1010 is important in the nylon family. Compared with nylon 6, it has better toughness at low temperature, self-lubrication, and lower water absorption ratio. Nylon 1010 has high crack initiation energy but low crack propagation energy and thus has high unnotched but low-notched impact strength and is also a pseudo-ductile polymer.[1] With increasing demands for high fracture-resistant nylon, much work has been done to improve the toughness especially to enhance the notched impact strength by using rubbers and their functional version such as maleated rubbers.[2–10] The effects of matrix molecule weight,[11–13] rubber functionality,[14–16] and rubber type[17–20] on the toughness of nylon were investigated. One problem of such rubber-toughened nylon is the stiffness of nylon, which usually decreases because of the low rigidity of rubber particles. Incorporation of inorganic fillers,[21–23] especially glass fiber (GF), is an effective way to remedy the decrease in stiffness.[24–30] Short fibers can improve the fracture toughness for brittle matrix composites like styrene acrylonitrile.[31,32] However, for ductile polymer matrix or rubber-toughened polymer, there is a remarkable decrease in toughness after the addition of these brittle fibers.[24,25,33,34] In most cases, the toughness of rubber-toughened nylon drops sharply with the addition of small amounts of GF and then is slightly enhanced with increasing GF content.[24,32] Therefore, there should be a trade-off between the toughness and stiffness of nylon by the incorporation of rubber toughening and GF reinforcing. Laura et al.[24] found that the decrease in toughness of rubber-toughened nylon 66 could be well compensated by the addition of 10 wt % GF.

In this work, the maleated poly(ethylene 1-octene) (POE-*g*-MAH) was used as impact modifier and GF as reinforcing filler to modify nylon 1010. The effects of GF content and the addition of rubber on the stiffness and toughness of nylon have been investigated. Besides the standard notched Izod impact test, the modified essential work of fracture (EWF) model was used to investigate the fracture behavior of nylon and its composites. The limited fracture energy and dissipative energy density were examined as a function of GF content, finding out how the GF content affects the toughness of rubber-toughened nylon 1010. The dispersion of rubber and GF as well as the tensile and impact fracture morphology were also investigated.

Correspondence to: Y. Zhang (yong_zhang@sjtu.edu.cn).
Contract grant sponsor: Shanghai Leading Academic Discipline Project; contract grant number: B202.

TABLE I
Recipe of Nylon/POE-*g*-MAH/GF Composites and the Corresponding Rubber Content Required in the Master Batch

Sample ID	POE-*g*-MAH[a] (wt %)	GF[b] (wt %)	Rubber content in master batch (wt %)
N-0-0	0	0	0
N-0-5	0	5	0
N-0-10	0	10	0
N-0-15	0	15	0
N-0-20	0	20	0
N-0-25	0	25	0
N-20-0	20	0	20
N-20-5	20	5	22.6
N-20-10	20	10	26.1
N-20-15	20	15	30.8
N-20-20	20	20	37.5
N-20-25	20	25	48

[a] POE-*g*-MAH content in nylon/POE-*g*-MAH blends.
[b] GF content based on nylon/POE-*g*-MAH blends.

EXPERIMENTAL

Nylon 1010 and GF-reinforced nylon 1010 used were manufactured by Shanghai Salient Chemical (Shanghai, China). POE-*g*-MAH was purchased from Shanghai Sunny New Technology Development Co., Ltd. (Shanghai, China), and the MAH grafting degree is about 0.5 wt %.

Processing

Nylon 1010 pellets were dried in a vacuum oven at 90°C for over 12 h, and POE-*g*-MAH was vacuum-dried at 60°C for 4 h. The preparation of GF-reinforced and rubber-toughened nylon 1010 is according to Laura's[24] method. First, a master batch blend containing nylon 1010 and POE-*g*-MAH with different weight ratios were prepared by using counter-rotating twin-screw extruder with a diameter of 25 mm and an L/D ratio of 41. The temperatures along the extruder were set at 195, 200, 205, 210, 210, 210, 210, 205°C. The rotor speed was 200 rpm. The standard tensile and Izod impact specimens were prepared according to the ISO R527 and ISO 180 in a plastic injection molding machine. The barrel temperatures were 205°C (hopper) and 220°C (nozzle), and the mold temperature was 45°C. The injection pressure was 40 MPa. Table I gives the required rubber content in master batches for nylon/POE-*g*-MAH/GF composites with different GF contents.

Mechanical testing

The tensile and flexural properties were measured using an Instron 4465 test machine at a crosshead speed of 50 and 2 mm/min according to ISO 527 and ISO 178, respectively. For GF-reinforced nylon composites, the crosshead speed of 5 mm/min was used in the tensile test. Notched Izod impact strength was tested using a Ray-Ran Universal Pendulum Impact Tester (UK) at a pendulum speed of 3.5 m/s according to ISO 180. Single-edge-notched three-point bending test (SEN3PB) specimens (Fig. 1) with dimensions of 80 × 10 × 4 mm^3 were cut from the injection-molded plaques. The notches of different depths (a) were first made by the formation of saw-cut slots having rectangular shape and then by sharpening with a fresh razor blade. The total crack length varied from 20 to 80% of the specimen width, and the ligament length (l) was measured from the original crack tip to the beginning of the hinge (Fig. 1). The total fracture energy was calculated according to the obtained impact strength and measured fracture area.

Morphology

Morphology of the blends was studied using field emission scanning electron microscopy (FESEM) (JSM-7401F JEOL, Japan). Images were taken from cryogenically fractured surfaces of specimens. The fracture morphology was directly taken from the tensile and impact fracture surface of samples. All the fractured surfaces were etched with toluene to remove the POE-*g*-MAH phase in nylon blends and composites, and then they were coated with gold before observation.

Dynamic mechanical analysis

Dynamic mechanical properties were measured using a rheometer DMTA IV from Rheometric Scientific (USA) under a single cantilever mode at a frequency of 1 Hz with dynamic strain of 0.01% in a temperature range of −80 to 140°C and at a heating rate of 3°C/min. Samples were made in the form of rectangular strips in dimensions of 30 × 4 × 2 mm^3.

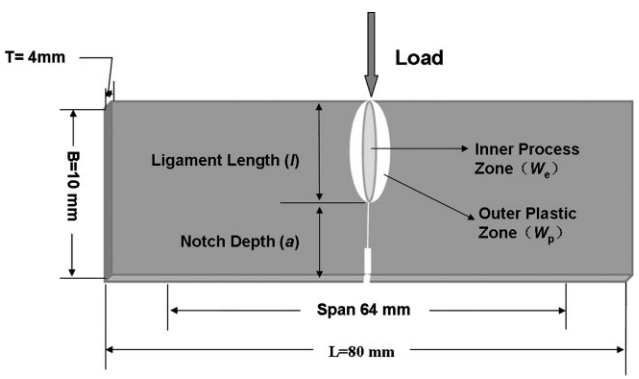

Figure 1 Single-edge notched specimen displaying width (B), thickness (T), ligament length (l), inner fracture process zone, and outer plastic zone.

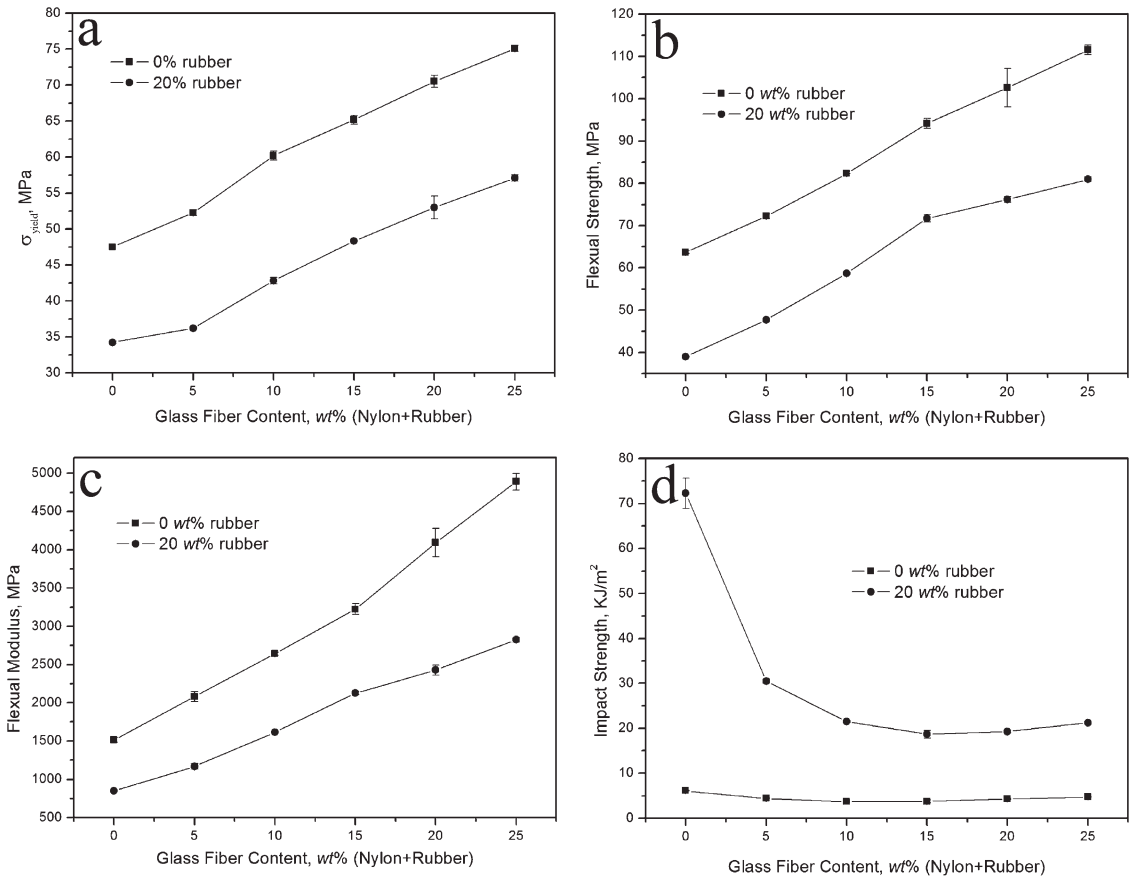

Figure 2 The mechanical properties of nylon/GF composites (■) and nylon/POE-*g*-MAH/GF (●) composites: (a) tensile yield strength; (b) flexural strength; (c) flexural modulus; and (d) impact strength.

RESULTS AND DISCUSSION

Mechanical properties

The yield strength, flexural strength, and modulus of nylon 1010 and its composites almost linearly increase with increasing GF content (Fig. 2). The yield strength increases to more than 60%, and the flexural modulus increases by 200% when the GF content is 25 wt %. The GF can effectively counteract the decrease in stiffness caused by the addition of 20 wt % POE-*g*-MAH. When the GF content is more than 10 wt %, the yield strength, flexural strength, and modulus of the nylon/POE-*g*-MAH/GF composites are higher than those of nylon 1010. The impact test shows nylon 1010 is very sensitive to the premade notch and has low notched impact strength (Fig. 2d). Nylon/POE-*g*-MAH (80/20) blend has much higher impact strength (more than 70 kJ/m^2) and is super tough. GF (5 wt %) causes a significant decrease in the impact strength. The embrittling effect of GF may be attributed to debonding at the interfaces between GF and nylon matrix as a result of stress concentration at their interfaces.[35] The impact strength of nylon/POE-*g*-MAH/GF composites is not dependent on the GF content when GF content is more than 5 wt %. The elongation at break of nylon/GF composites decreases with increasing GF content and drops to less than 5% when the GF content is more than 10 wt %. At a given GF content, the nylon/POE-*g*-MAH/GF composites have higher elongation at break than their corresponding nylon/GF composites (Table II).

Fracture behavior

The standard notched Charpy and Izod impact tests are commonly used to characterize the toughness of polymer materials in modern industry because of their simple convenient test methods. However,

TABLE II
Elongation at Break of GF-Reinforced Nylon and Their Rubber-Toughened Counterparts

GF content[a] (wt %)	0	5	10	15	20	25
ε_b (%, 0 wt % rubber[b])	285	25.9	5.2	4.0	4.0	3.7
ε_b (%, 20 wt % rubber[b])	247	46.2	15.6	8.7	7.3	6.3

[a] POE-*g*-MAH content in nylon/POE-*g*-MAH blends.
[b] GF content based on nylon/POE-*g*-MAH blends.

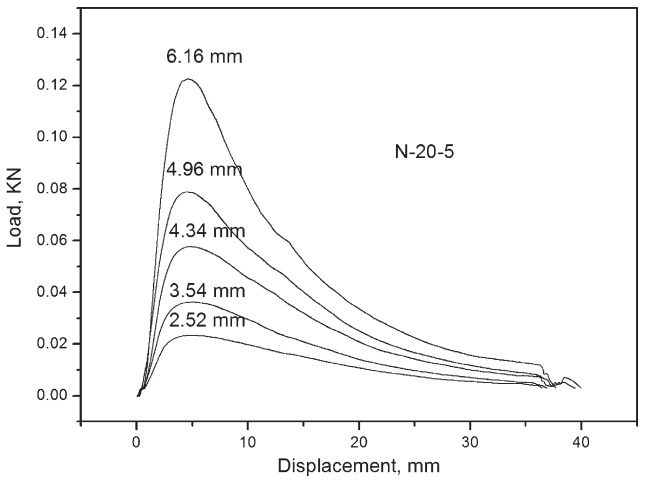

Figure 3 Load-displacement curves for specimens of nylon/POE-*g*-MAH/GF (80/20/5) composite.

these standard impact tests also have several drawbacks. They are limited to specimens with a specific notch geometry and a given fracture area, merely reveal the energy dissipation during the whole test and fail to provide a general representation of the toughness of materials.[36] Hence, several fracture mechanic techniques such as J-integral[34] and linear elastic fracture mechanics (LEFM) method[37,38] have been proposed to characterize the fracture behavior of materials. However, the J-integral method cannot be widely used for its implementation requiring specialized equipments and rigorous treatment for specimens. On the other hand, the LEFM method fails to characterize the fracture behavior of samples with a nonlinear zone, usually an outer plastic zone. The EWF model proposed by Mai and coworkers[34,39,40] has been successfully used to characterize the fracture behavior of rubber-toughened and/or GF-reinforced materials.[34,36,41–46] According to the EWF model, the total fracture energy (W_f) mainly includes two parts: the surface-related fracture work (W_e) of the polymer in the inner fracture process zone and the volume-related energy (W_p) consumed by various deformation mechanisms in the plastic zone[36] [eq. (1)]. W_e is the EWF, whereas W_p is the nonessential one. The EWF model can be expressed in the following equations:

$$W_f = W_e + W_p \tag{1}$$

$$W_f = w_e l T + \beta w_p l^2 T \tag{2}$$

$$w_f = W_f / lT = w_e + \beta w_p l \tag{3}$$

where l is the ligament length, T is the thickness of specimen, β is a shape factor of the plastic zone, w_f is the specific total fracture energy, w_e is the specific EWF, and βw_p is the specific nonessential plastic work. This method is a simple method to reveal the fracture behavior of materials. T and l can be directly measured, whereas W_f can be calculated by the area of the given load-displacement curves. Then, w_f is linearly fitted with the ligament length l. The slope of the fitted line is βw_p and the intersection is w_e. Several requirements must be satisfied before the implementation of this EWF method. First, the specimen ligament must be fully yielded before crack growth; second, the essential fracture work W_e consumed in the inner fracture process zone is proportional to l; last, volume of outer plastic zone must be proportional to the square of ligament length (l^2).[47]

In this article, the modified EWF model is used because the two parts of specimens could not be completely separated after the SEN3PB testing. Therefore, the actual ligament length l used in the test is the length of stress whitening zone in the fracture direction. In this modified EWF model, the total fracture energy (U), unit fracture surface area (A), is given by

$$U/A = u_0 + u_d l \tag{4}$$

where u_0 is the limited specific fracture energy corresponding to the intersection of the fitted line of U/A and l, and u_d is the dissipative energy density corresponding to the slope. Unlike w_e and βw_p, u_0 and u_d are defined as phenomenological rather than material parameters.[25,48]

The load-displacement curves of nylon/POE-*g*-MAH/GF (80/20/5 and 80/20/25) composites with different ligament lengths are shown in Figures 3 and 4, respectively. All the curves look similar indicating the geometry similarity during the growth of crack between samples with different l. All SEN3PB

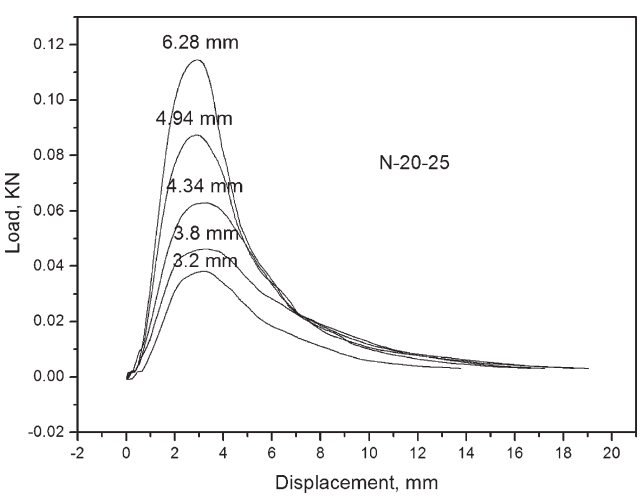

Figure 4 Load-displacement curves for specimens of nylon/POE-*g*-MAH/GF (80/20/25) composite of different ligament lengths.

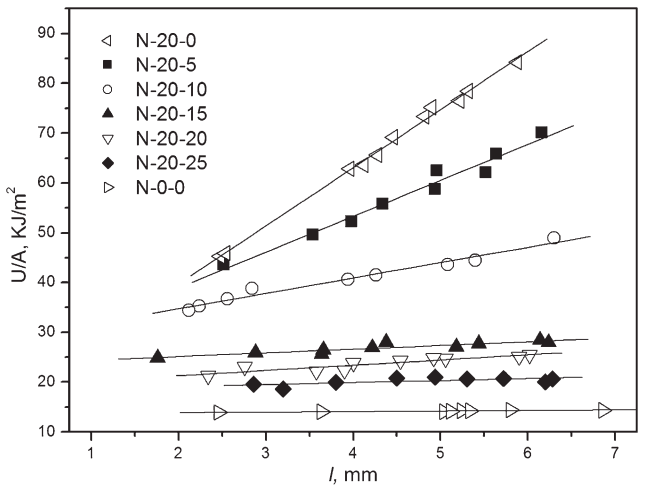

Figure 5 U/A versus l for nylon and nylon/POE-*g*-MAH/GF composites.

test will be automatically stopped when the load drops below a threshold value (3 N). For the nylon/POE-*g*-MAH/GF (80/20/5) composite, the load reaches the maximum value and slowly decreases to the threshold value thereafter, indicating the samples are rather ductile. For nylon/POE-*g*-MAH/GF (80/20/25) composite, the load decreases to the threshold value from the maximum load with less decay, indicating that the crack propagation is fast with less energy absorption in comparison with that of the nylon/POE-*g*-MAH/GF (80/20/5) composite and the former is pretty brittle. The total fracture energy of samples is calculated by integrating their corresponding load–displacement curves.

The U/A for nylon and its composites is plotted versus l (Fig. 5). For all the samples examined, good linearity was obtained. The slope (u_d) is associated with the energy consumption in the outer plastic zone away from the process zone (Fig. 1).[25] The slope of $U/A \sim l$ plot of nylon 1010 is almost zero (Fig. 5), suggesting that the total fracture energy is mainly dissipated in the inner fracture process zone (Fig. 1) and little energy is dissipated in the outer plastic zone. For the nylon/POE-*g*-MAH (80/20) blend, both u_0 and u_d are much higher in comparison with pristine nylon. The addition of POE-*g*-MAH significantly increases the energy dissipation in crack propagation and plastic deformation. The u_d decreases significantly after the addition of GF. With increasing GF content, u_d gradually decreases to near zero and then reaches a plateau, suggesting that there is little energy consumed in the outer plastic zone, which is well related to the observed phenomenon. With increasing GF content, the thickness of the stress-whitening zone gradually decreases during the SEN3PB test. The u_0 increases to the maximum value at the GF content of 10 wt % and then sharply decreases with increasing GF content (Fig. 6). The energy absorption mechanisms for polymer are mainly bulk matrix yielding and plastic deformation of the fiber/matrix interphase, whereas the GF-related energy absorption mechanisms mainly lie on fiber fracture, debonding, and pull out.[34] GF has a much higher modulus than nylon, which will produce high stress concentrations at their interfaces and enhance the plasticity in the surrounding matrix, reduce the hydrostatic stress state, and increase the deviatoric stress.[35,49] Hence, u_0 can be further increased in the presence of small amounts of fiber. On the other hand, the constraining effect of GF may prevent matrix from yielding and reduce the volume of fracture process zone. With increasing GF content, this constraining effect becomes more pronounced and therefore u_0 is sharply decreased. The nylon/POE-*g*-MAH (80/20) blend has the largest u_d while the nylon/POE-*g*-MAH/GF (80/20/10) composite has the largest u_0, but the former is much tougher than the latter. Therefore, it is u_d rather than u_0 that mainly accounts for the high level of toughness.

Morphology

All the samples were subjected to brittle fracture in liquid nitrogen and the fracture surfaces were etched in toluene at its boiling temperature for 2 h to remove the POE-*g*-MAH phase, and therefore the holes left on the fracture surface can reflect the phase domain of POE-*g*-MAH. The fracture surface of nylon 1010 is smooth with no holes [Fig. 7(a)] because nylon is insolvable in boiling toluene. GF is dispersed in the nylon matrix with a diameter about 13 μm and is highly oriented [Fig. 7(b)]. The POE-*g*-MAH particles in the nylon/POE-*g*-MAH (80/20) blend are uniformly dispersed as spherical particles on the nylon matrix with an average diameter of about 0.2 μm [Fig. 7(c)]. GF has little effect on the

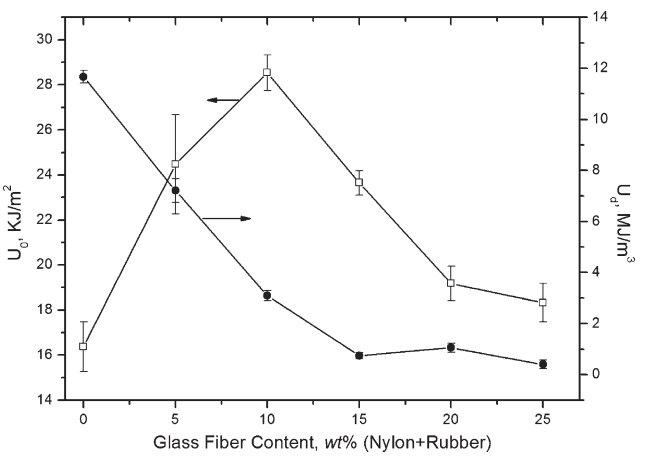

Figure 6 u_0 and u_d for nylon/POE-*g*-MAH/GF composites as a function of GF content.

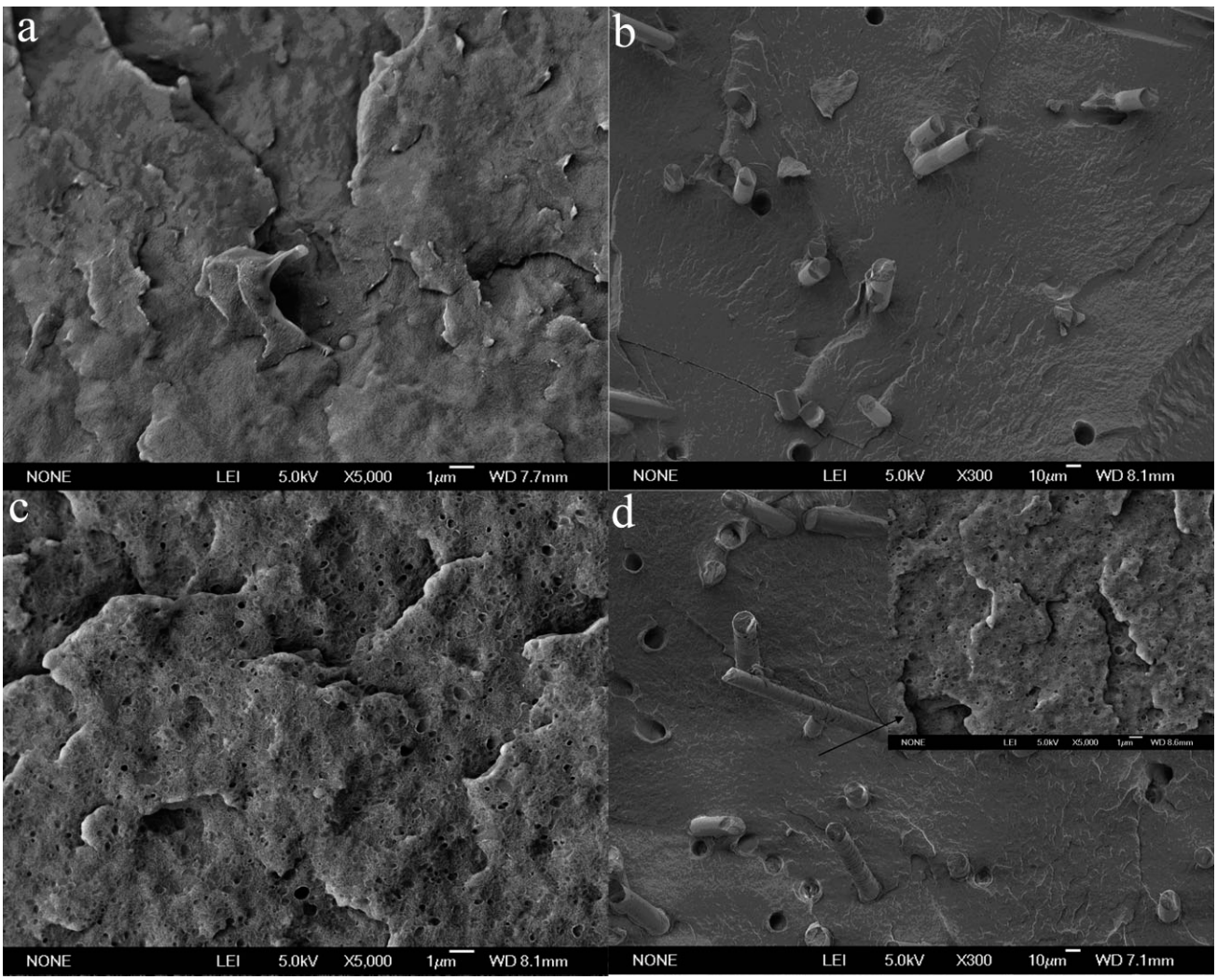

Figure 7 SEM images of nylon, nylon/POE-*g*-MAH blend, and their GF-reinforced composites: (a) N-0-0; (b) N-0-10; (c) N-20-0; and (d) N-20-10.

dispersion of POE-*g*-MAH in nylon 1010. The rubber particles are still spherical with a comparable particle size with that in the nylon/POE-*g*-MAH (80/20) blend [Fig. 7(d)].

The impact fracture surface of nylon/POE-*g*-MAH (80/20) blend and its GF-reinforced counterpart has been investigated. To observe the whole fracture surface, two images at low magnification were merged, and the arrow indicates the fracture direction in impact test [Fig. 8(a,c)]. The fracture surface of nylon/POE-*g*-MAH/GF (80/20/5) composite is very rough [Fig. 8(c)]. The similar fracture morphology is observed at both the place near the notch and far from the notch. For the nylon/POE-*g*-MAH (80/20) blend, the fracture surface is smooth at low magnification [Fig. 8(a)]. Further observation shows that the POE-*g*-MAH particles have been stretched to ellipsoidal ones [Fig. 8(b)] and the matrix around suffers a large plastic deformation, which are totally different from that obtained in liquid nitrogen [Fig. 7(c)]. For the nylon/POE-*g*-MAH/GF (80/20/5) composite, large plastic deformation of nylon 1010 matrix is found around the GF instead of POE-*g*-MAH particles [Fig. 8(d,e)]. In case of the nylon/POE-*g*-MAH (80/20) blend, with an outer force applied, the rubber particles are prone to cavitation, and matrix around those cavitated particles may suffer a great plastic deformation because of the high stress concentration in the nylon/rubber interphase [Fig. 8(b)], which plays a main role in energy dissipation. Therefore, the blend is super tough. In case of the nylon/POE-*g*-MAH/GF (80/20/5) composite, GF can probably produce higher stress concentration in comparison with POE-*g*-MAH particles. Hence, large matrix plastic deformation is observed around GF instead of POE-*g*-MAH.

Figure 9 shows the morphology of tensile fracture surface and the surface, which is near the fracture surface but parallel to the tensile direction of the nylon/POE-*g*-MAH/GF (80/20/5) composite. There is

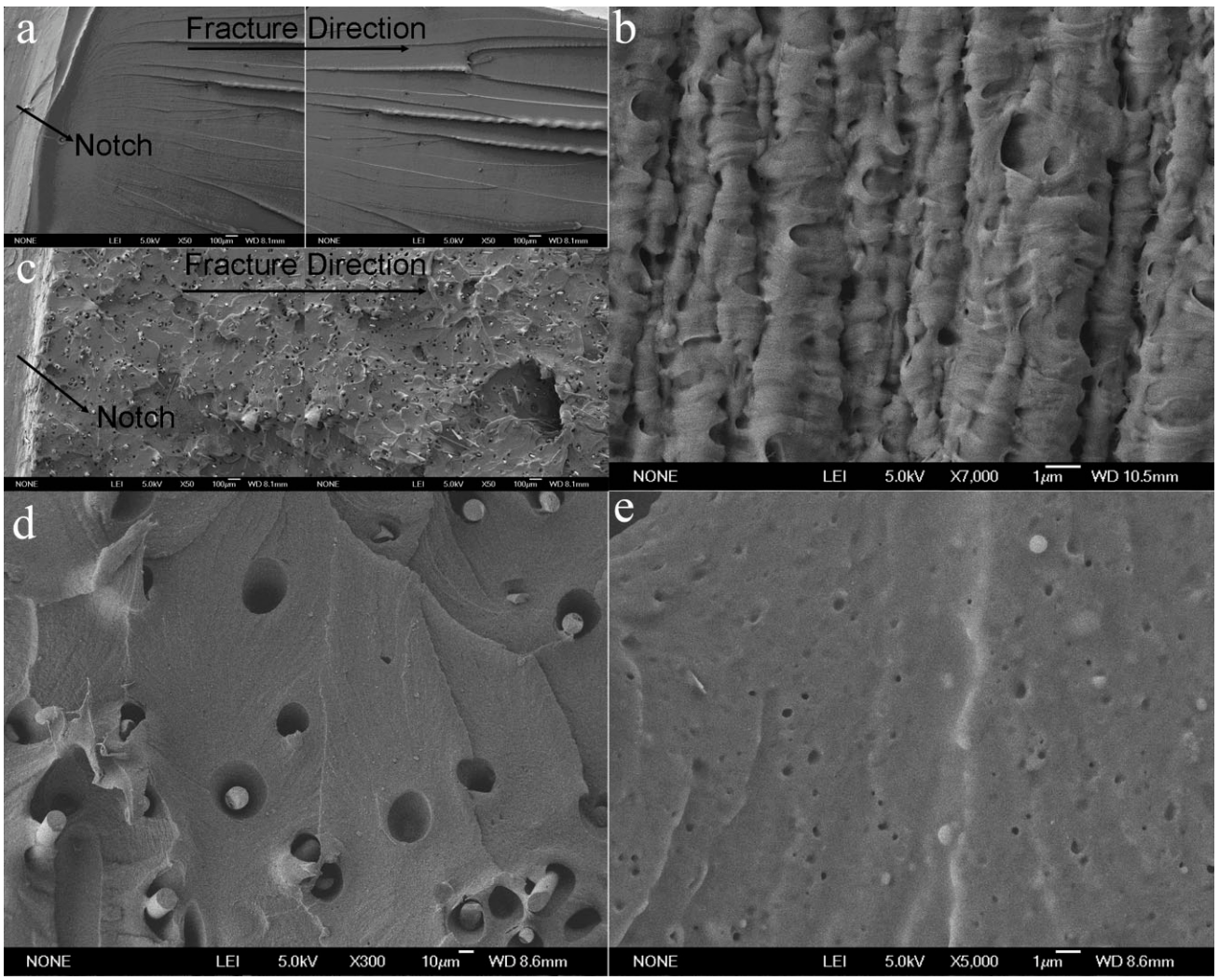

Figure 8 Impact fracture morphology of the nylon/POE-*g*-MAH (80/20) blend and nylon/POE-*g*-MAH/GF (80/20/5) composite. (a) and (b): N-20-0; (c), (d), and (e): N-20-5.

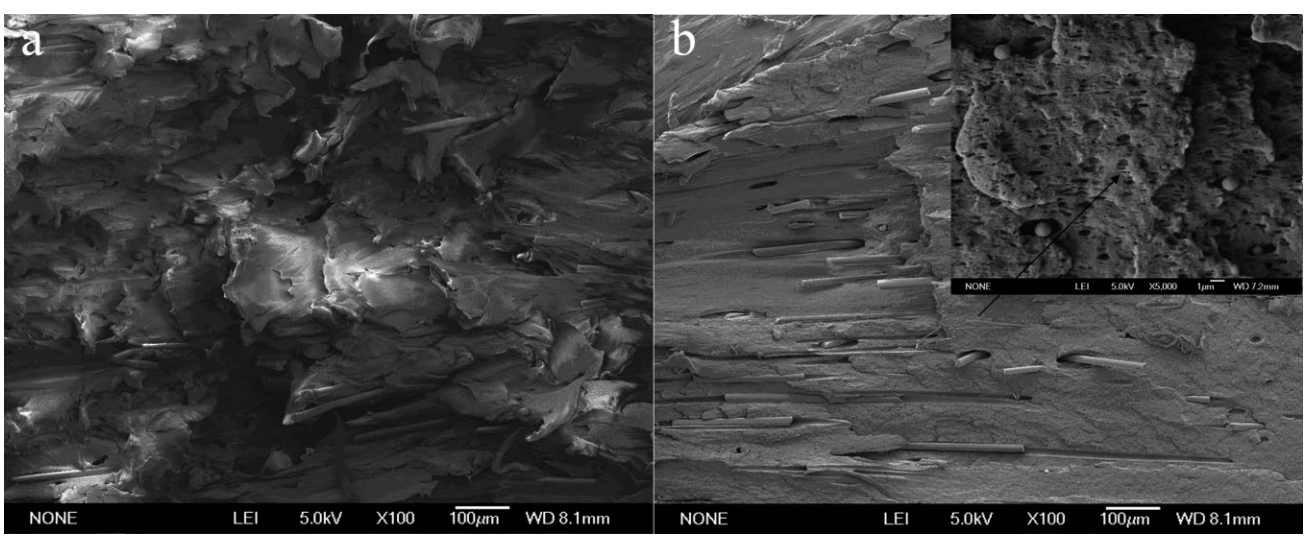

Figure 9 Tensile fracture morphology of nylon/POE-*g*-MAH/GF (80/20/5) composite: (a) tensile fracture surface and (b) fracture surface along with the tensile direction obtained in liquid nitrogen.

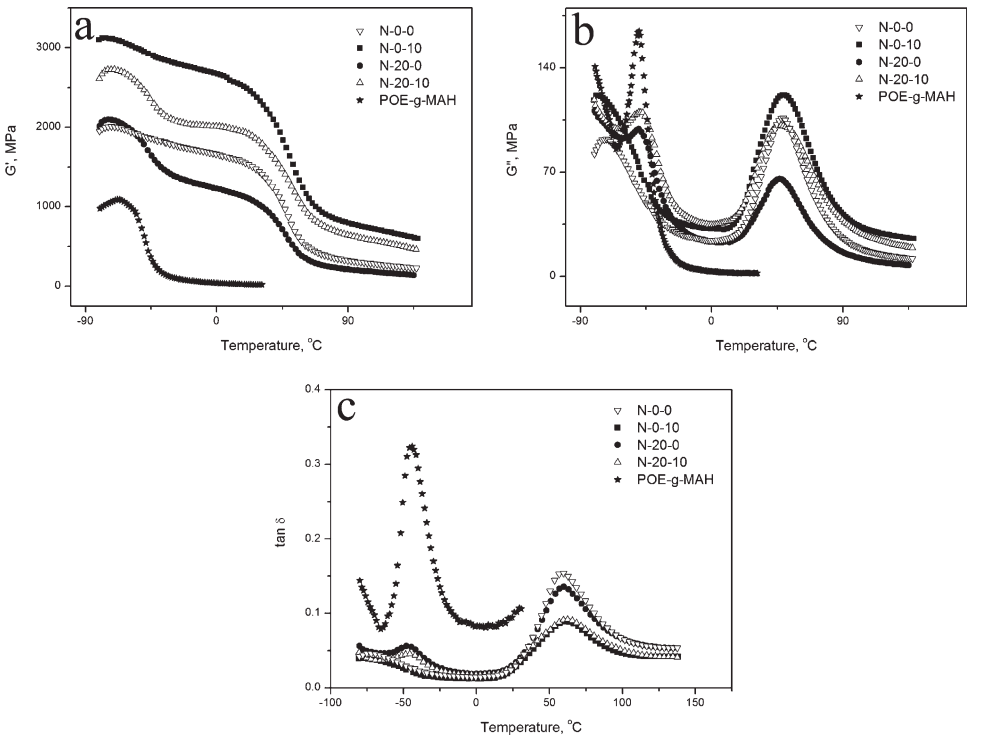

Figure 10 Dynamic mechanical properties of nylon blends: (a) storage modulus (G'); (b) loss modulus (G''); and (c) loss factor (tan δ).

an obvious plastic deformation on the fracture surface [Fig. 9(a)], suggesting a significant bulk matrix yielding in the tensile test. Holes left on the surface are attributed to the pull out of GF caused by the void formation at fiber ends. Almost all the GF observed is aligned with the tensile direction, indicating a high orientation [Fig. 9(b)]. The POE-*g*-MAH particles have been stretched along the tensile direction as ellipsoidal particles. The rubber particles on the fracture surface have been hardly stretched during the impact test with a high loading rate of 3.5 m/s. However, in the tensile test, the rubber particles can be fully stretched under quasi-static rate of loading ($v = 5$ mm/min). Therefore, the fracture morphology under dynamic and quasi-static state is totally different.

Dynamic mechanical properties

The cavitation of rubber particles, which can release the triaxial stress and trigger the shear yielding of matrix especially the pseudo-ductile polymers, has been emphasized. The relative ease of rubber particles cavitation certainly depends on the shear moduli of both matrix and rubber phase. It was reported that when the shear moduli ratio of dispersed phase to the matrix is less than one-tenth, the dispersed rubber particles will act as an effective impact modifier.[17] Hence, it is necessary to examine the variation of moduli toward temperature, from which the brittle–ductile temperature can be estimated. Dynamic mechanical analysis (DMA) provides a convenient way to examine the changes of moduli toward temperature (Fig. 10). According to the criterion discussed earlier, the brittle–ductile transition temperature of the nylon/POE-*g*-MAH (80/20) blend should be about −40°C, below which the moduli ratio of POE-*g*-MAH to nylon 1010 matrix is over one-tenth [Fig. 10(a)]. The addition of GF into nylon leads to an obvious increase in storage modulus (G') no matter whether POE-*g*-MAH exists [Fig. 10(a)]. The decrease in G' of nylon/POE-*g*-MAH (80/20) and nylon/POE-*g*-MAH/GF (80/20/10) at around −50°C is attributed to the glass transition of POE-*g*-MAH. The peak value of loss modulus (G) at around 50°C is increased by the addition of GF but decreased by the addition of POE-*g*-MAH [Fig. 10(b)]. The peak observed at about −50°C in G curves of the nylon/POE-*g*-MAH (80/20) blend and nylon/POE-*g*-MAH/GF (80/20/10) composite is probably attributed to the relaxation of POE-*g*-MAH. The tan δ curve shows the glass transition occurs at around 60°C for nylon and −45°C for POE-*g*-MAH [Fig. 10(c)]. GF has less effect on the glass transition temperatures of nylon and POE-*g*-MAH but can significantly decrease the tan δ value of nylon.

CONCLUSIONS

Nylon 1010 was effectively toughened by POE-*g*-MAH and nylon 1010 with high impact strength (over 70 kJ/m^2) was obtained by blending with

20 wt % POE-*g*-MAH. GF significantly enhanced the stiffness of nylon and its blends. With increasing GF content, the yield strength and flexural modulus gradually increased. The decrease in stiffness caused by the addition of POE-*g*-MAH could be well compensated at the GF content more than 10 wt %. The impact strength of nylon/POE-*g*-MAH (80/20) blend decreased by more than 50% after the addition of 5 wt % GF. With increasing GF content, the impact strength slightly decreased and reached a plateau when GF content was more than 10 wt % but was still much higher than that of nylon 1010.

The modified EWF model was used to characterize the fracture behavior of nylon and its composites. With increasing GF content, the dissipative energy density (u_d) gradually decreased, suggesting a decreasing energy consumed in the outer plastic zone. It was corresponding with the observed phenomenon that the thickness of the outer plastic zone in SEN3PB test decreased with increasing GF content. The limited specific fracture energy (u_0) increased with increasing GF content at first, reached the maximum value when the GF content was 10 wt % and then decreased thereafter. For the nylon/POE-*g*-MAH (80/20) blend, FESEM showed matrix around the POE-*g*-MAH particles suffered a great plastic deformation in the impact test. However, in the nylon/POE-*g*-MAH/GF (80/20/5) composite, large plastic deformation was found in the nylon matrix around GF instead of POE-*g*-MAH particles. The fracture morphology of nylon/POE-*g*-MAH/GF (80/20/5) composite depended on the test modes. The rubber particles were stretched to ellipsoidal in the tensile test (quasi-static test) but were still spherical in the impact test (dynamic test). The storage and loss moduli of nylon and the nylon/POE-*g*-MAH (80/20) blend obtained in DMA with a single cantilever mode increased after the addition of GF. The introduction of GF decreased the loss factor value at the T_g of nylon 1010 but had less effect on the position of T_g of nylon and POE-*g*-MAH.

References

1. Wang, X.-H.; Zhang, H.-X.; Jiang, W.; Wang, Z.-G.; Liu, C.-H.; Liang, H.-J.; Jiang, B.-Z. Polymer 1998, 39, 2697.
2. Sun, S. L.; Tan, Z. Y.; Xu, X. F.; Zhou, C.; Ao, Y. H.; Zhang, H. X. J Polym Sci Part B: Polym Phys 2005, 43, 2170.
3. Shalaby, S. E.; Al-Balakocy, N. G.; Abo El-Ola, S. M. J Appl Polym Sci 2006, 99, 613.
4. Sui, G. X.; Wong, S. C.; Yang, R.; Yue, C. Y. Compos Sci Technol 2005, 65, 221.
5. Filippi, S.; Minkova, L.; Dintcheva, N.; Narducci, P.; Magagnini, P. Polymer 2005, 46, 8054.
6. Yu, Z. Z.; Ou, Y. C.; Qi, Z. N.; Hu, G. H. J Polym Sci Part B: Polym Phys 1998, 36, 1987.
7. Lai, S. M.; Liao, Y. C.; Chen, T. W. J Appl Polym Sci 2006, 100, 1364.
8. Chen, H.; Yang, B.; Zhang, H. J Appl Polym Sci 2000, 77, 928.
9. Lu, M.; Keskkula, H.; Paul, D. R. J Appl Polym Sci 1996, 59, 1467.
10. Lu, M.; Keskkula, H.; Paul, D. R. J Appl Polym Sci 1995, 58, 1175.
11. Oshinski, A. J.; Keskkula, H.; Paul, D. R. Polymer 1996, 37, 4891.
12. Oshinski, A. J.; Keskkula, H.; Paul, D. R. Polymer 1996, 37, 4909.
13. Oshinski, A. J.; Keskkula, H.; Paul, D. R. Polymer 1996, 37, 4919.
14. Wong, S. C.; Mai, Y. W. Key Eng Mater 1998, 137, 55.
15. Wong, S. C.; Mai, Y. W. Polymer 1999, 40, 1553.
16. Wong, S.-C.; Mai, Y.-W. Polymer 2000, 41, 5471.
17. Huang, J. J.; Keskkula, H.; Paul, D. R. Polymer 2006, 47, 639.
18. Huang, J. J.; Keskkula, H.; Paul, D. R. Polymer 2006, 47, 624.
19. Huang, J. J.; Paul, D. R. Polymer 2006, 47, 3505.
20. Burgisi, G.; Paternoster, M.; Peduto, N.; Saraceno, A. J Appl Polym Sci 1997, 66, 777.
21. Tohgo, K.; Fukuhara, D.; Hadano, A. Compos Sci Technol 2001, 61, 1005.
22. Ahn, Y.-C.; Paul, D. R. Polymer 2006, 47, 2830.
23. Dong, W.; Zhang, X.; Liu, Y.; Gui, H.; Wang, Q.; Gao, J.; Song, Z.; Lai, J.; Huang, F.; Qiao, J. Eur Polym J 2006, 42, 2515.
24. Laura, D. M.; Keskkula, H.; Barlow, J. W.; Paul, D. R. Polymer 2000, 41, 7165.
25. Laura, D. M.; Keskkula, H.; Barlow, J. W.; Paul, D. R. Polymer 2003, 44, 3347.
26. Huerta-Martinez, B. M.; Ramirez-Vargas, E.; Medellin-Rodriguez, F. J.; Garcia, R. C. Eur Polym J 2005, 41, 519.
27. Li, L.; Li, B.; Tang, F. Eur Polym J 2007, 43, 2604.
28. Seo, Y.; Hwang, S. S.; Kim, K. U.; Lee, J.; Li, S. H. Polymer 1993, 34, 1667.
29. Fu, S. Y.; Lauke, B.; Zhang, Y. H.; Mai, Y. W. Compos A 2005, 36, 987.
30. Whan, C. J.; Paul, D. R. J Appl Polym Sci 2001, 80, 484.
31. Akay, M.; O'Regan, D. F.; Bailey, R. S. Compos Sci Technol 1995, 55, 109.
32. Nair, S. V.; Wong, S. C.; Goettler, L. A. J Mater Sci 1997, 32, 5335.
33. Laura, D. M.; Keskkula, H.; Barlow, J. W.; Paul, D. R. Polymer 2002, 43, 4673.
34. Ching, C. Y.; Li, K. Y.; Tjong, S. C.; Mai, Y.-W. Polym Eng Sci 2003, 43, 558.
35. Nair, S. V.; Subramaniam, A.; Goettler, L. A. J Mater Sci 1997, 32, 5347.
36. Bao, S. P.; Tjong, S. C. Compos A 2007, 38, 378.
37. Laura, D. M.; Keskkula, H.; Barlow, J. W.; Paul, D. R. Polymer 2001, 42, 6161.
38. Fung, K. L.; Li, R. K. Y. Polym Test 2005, 24, 863.
39. Wu, J.; Mai, Y.-W. Polym Eng Sci 1996, 36, 2275.
40. Marshall, G. P.; Williams, J. G.; Turner, C. E. J Mater Sci 1973, 8, 949.
41. Lach, R.; Schneider, K.; Weidisch, R.; Janke, A.; Knoll, K. Eur Polym J 2005, 41, 383.
42. Costa, F. R.; Satapathy, B. K.; Wagenknecht, U.; Weidisch, R.; Heinrich, G. Eur Polym J 2006, 42, 2140.
43. Gong, G.; Xie, B. H.; Yang, W.; Li, Z. M.; Lai, S. M.; Yang, M. B. Polym Test 2006, 25, 98.
44. Tjong, S. C.; Bao, S. P. J Polym Sci Part B: Polym Phys 2005, 43, 585.
45. Tjong, S.-C.; Xu, S.-A.; Mai, Y.-W. J Polym Sci Part B: Polym Phys 2002, 40, 1881.
46. Tjong, S. C.; Xu, S. A.; Li, R. K. Y.; Mai, Y. W. J Appl Polym Sci 2002, 87, 441.
47. Fasce, L.; Bernal, C.; Frontini, P.; Mai, Y.-W. Polym Eng Sci 2001, 41, 1.
48. Zhang, S.; Chen, G.; Cui, C.; Mi, C.; Gu, J.; Yu, J. Fuhe Cailiao Xuebao/Acta Mater Compos Sinica 2006, 23, 31.
49. Ming-Liang, S.; Nair, S. V.; Garrett, P. D.; Pollard, R. E. Polymer 1994, 35, 306.